FEBS Letters 589 (2015) 2763–2768

journal homepage: www.FEBSLetters.org

Asymmetries in kinesin-2 and cytoplasmic dynein contributions to melanosome transport

María Cecilia De Rossi [a], María Emilia De Rossi [b], Mariela Sued [c], Daniela Rodríguez [c], Luciana Bruno [d,*], Valeria Levi [a,*]

[a] Departamento de Química Biológica, Facultad de Ciencias Exactas y Naturales, Universidad de Buenos Aires, IQUIBICEN-CONICET, Ciudad Universitaria, CP1428 Ciudad de Buenos Aires, Argentina
[b] Instituto de Astronomía y Física del Espacio, Universidad de Buenos Aires-CONICET, Ciudad Universitaria, CP1428 Ciudad de Buenos Aires, Argentina
[c] Instituto de Cálculo, Universidad de Buenos Aires-CONICET, Ciudad Universitaria, CP1428 Ciudad de Buenos Aires, Argentina
[d] Departamento de Física, Facultad de Ciencias Exactas y Naturales, Universidad de Buenos Aires, IFIBA-CONICET, Ciudad Universitaria, CP1428 Ciudad de Buenos Aires, Argentina

ARTICLE INFO

Article history:
Received 28 April 2015
Revised 17 July 2015
Accepted 20 July 2015
Available online 3 August 2015

Edited by Dietmar J. Manstein

Keywords:
Single particle tracking
Molecular motors
Intracellular transport
Xenopus laevis melanophores

ABSTRACT

The mechanisms involved in bidirectional transport along microtubules remain largely unknown. We explored the collective action of kinesin-2 and dynein motors during transport of melanosomes in *Xenopus laevis* melanophores. These motors are attached to organelles through accessory proteins establishing a complex molecular linker. We determined both the stiffness of this linker and the organelles speed and observed that these parameters depended on the organelle size and cargo direction. Our results suggest that melanosome transport is driven by two dissimilar teams: whereas dynein motors compete with kinesin-2 affecting the properties of plus-end directed organelles, kinesin-2 does not seem to play a similar role during minus-end transport.

1. Introduction

Molecular motors hydrolyze ATP to step along microtubules and actin filaments in eukaryotic cells. These molecules are responsible for the transport of a wide variety of cellular components and thus are essential for the intracellular trafficking and organization (reviewed in [1,2]).

Single particle/molecule techniques applied to isolated motors [3] or cellular systems [4–7] have provided valuable information about the biophysical properties of these nanomachines. These studies firmly demonstrated that organelles attach many copies of different motors [4–7]. In particular, the opposed-polarity microtubule motors kinesin and dynein are both simultaneously present on organelles actively moving toward the plus or minus end of microtubules [8] posing the question about how these motors work together during transport. Understanding the collective behavior of identical and opposed polarity motors is essential to get insight into the rules regulating the intracellular organization in both physiological and pathological conditions.

Two models were postulated to address multimotor behavior: the coordination model which proposes that there is a mechanism that switch on/off different sets of motors [9–11], and the tug-of-war model that postulates a competition between opposed-polarity motors, the stronger team wins the competition and defines the direction of the cargo [8,12]. Whereas there are evidences supporting both models, it is currently accepted that there is a complex interplay between local tug-of-war interactions on the cargos and larger regulatory events that bias the output of the tug-of-war (for a recent review see [13]).

Melanophore cells are one of the most widely used cellular systems for the study of intracellular transport [14]. These cells have pigmented organelles called melanosomes that can be easily observed using brightfield microscopy. Melatonin and MSH trigger signaling cascades that lead to the aggregation of melanosomes within the perinuclear region or their dispersion through the cytoplasm, respectively [15–21]. To achieve these configurations, melanosomes are transported along microtubules by action of the

Abbreviations: SPT, single particle tracking; κ, effective elastic constant; r_{op}, optical radius

Author contributions: MC de Rossi acquired and analyzed data; MC de Rossi, LB and VL contributed on the conception and design of the study; LB performed the numerical simulations, MC de Rossi, ME de Rossi, MS, DR, LB and VL performed the analysis and interpretation of the data, MC de Rossi, LB and VL wrote the manuscript.

* Corresponding authors. Fax: +54 114 786 3426.
E-mail addresses: lbruno@df.uba.ar (L. Bruno), vlevi12@gmail.com (V. Levi).

http://dx.doi.org/10.1016/j.febslet.2015.07.038
0014-5793/

cytoplasmic dynein [22] and kinesin-2 [23], whereas myosin V is responsible for actin dependent transport [24].

It is well known that certain properties of melanosome trajectories change during aggregation and dispersion (e.g. [7,25,26]). However, we still do not have a complete view on the molecular mechanisms involved in this regulation of transport that may include chemical modifications of the motors such as phosphorylation [18], changes on the motor interactions with adaptor or scaffolding proteins (reviewed in [27]), changes in the number of motor engaged in the transport [7,28] and modifications in the microtubule tracks [29].

Cargoes actively transported by motors experience a viscoelastic drag in the cytoplasm [30–35]. In this sense, small vesicles are expected to move faster, present higher run lengths and directionality. However, several experimental evidences suggest that these transport properties are also influenced by the number of active motors attached to the organelle [26,36,37]. Particularly, we have recently found that the tortuosity of the trajectories of melanosomes depends inversely on the organelle size [26]. We hypothesized that this effect could be explained considering that bigger organelles linked more motors and thus are less prone to detach from the track. This effect was more relevant in the case of minus-end directed organelles since dyneins easily detach from the track [12,38].

As we mentioned before, molecular motors are attached to organelles through accessory proteins which also play a relevant role in their function (reviewed in [20,39–42]). Dynactin seems to be a key player on defining microtubule-dependent transport of melanosomes. It links both, cytoplasmic dynein and kinesin-2 to the organelles through its $p150^{Glued}$ subunit and its disruption inhibits plus- and minus-end transport [43]. This complex is fundamental for the processivity of both dynein (reviewed in [44]) and kinesin-2 [45]. Dynactin improves dynein performance by increasing the average forward-step size, suppressing backward steps, and decreasing the overall probability of motor detachment from the microtubule per step [46]. Unfortunately, we do not have a detailed description regarding the influence of dynactin on kinesin-2 transport properties.

The motor linker established between organelle and microtubule has its characteristic stiffness and influence the transport behavior i.e. a stiff linker determines that the motion of the motor and organelle are highly correlated contrary to what it would be expected for a flexible linker.

We have recently shown that this mechanical property can be estimated in living cells by analyzing the organelle jittering perpendicular to the microtubule axis, e.g. the jittering amplitude is higher for more flexible linkers [47]. Moreover, numerical simulations showed that this intrinsic flexibility is very relevant to prevent the fast detachment of motors in a tug of war context [48].

In this work, we use this analysis tool to measure the mechanical properties of the motor linker attaching melanosomes of different sizes in order to understand the regulation of organelle transport driven by multiple copies of motors.

2. Materials and methods

2.1. Cell culture and sample preparation for imaging

Immortalized *Xenopus laevis* melanophores were cultured as described in [49]. Cells were grown in 70% L-15 medium (Sigma–Aldrich) supplemented with phenylthiourea [25] to reduce the amount of melanosomes for tracking experiments. For microscopy measurements, cells were plated for 2 days on 25-mm round coverslips placed into 35-mm dishes in 2.0 ml of complete medium. Before observation, the coverslips were washed in serum-free medium and mounted in a custom-made chamber specially designed for the microscope where the cells were incubated with 10 mM of Latrunculin B (Sigma–Aldrich) for 30 min to depolymerize actin filaments. Subsequently, hormonal stimulation for aggregation or dispersion was performed using 10 nM melatonin or 100 nM MSH, respectively [25]. Samples were observed during 15 min after stimulation.

2.2. Tracking experiments

Single particle tracking experiments were carried out in a Nikon Eclipse TE300 fluorescence microscope adapted for SPT using a 60× oil-immersion objective (NA: 1.35). A high-speed CCD camera (DVC 340 M, Thorlabs Inc.) was coupled to the video port of the microscope for imaging the cells. We recorded movies (2000 frames) of individual melanosomes at a speed of 300 frames/s and recovered the trajectories of the organelles with an accuracy in the range of 4–7 nm using the pattern recognition tracking method previously described [7].

2.3. Measurement of the motor linker stiffness

The determination of the effective elastic constant (κ) was performed following a spring-like-interaction model based on the generalized Langevin equation [47] with some modifications. Briefly, curvilinear sections of trajectories were selected and divided into segments of 0.39 s of duration (130 data points). These segments were fitted with a second order polynomial function to obtain the position fluctuations perpendicular to the main transport direction ($y_\perp$).

The mean squared displacement of motion perpendicular to the transport direction ($MSD_\perp$) was calculated as:

$$MSD_\perp(\tau) = < (y_\perp(t+\tau) - y_\perp(t))^2 > \quad (1)$$

where t and τ correspond to the absolute and lag times, respectively and the brackets indicate the time average.

We computed the asymptotic MSD (∞) by averaging $MSD_\perp$ in the interval $0.12\ s < \tau < 0.27\ s$ and calculated the elastic constant κ as:

$$\kappa = \frac{2K_B T}{MSD(\infty) - 2\delta^2} \quad (2)$$

where K_B and T corresponds to the Boltzmann constant and the absolute temperature (298 K), respectively and δ is the error in the determination of melanosome position.

These routines were programed using IDL (Interactive Data Language).

2.4. Statistical analysis

For each data group g, we computed the median med(g) since the data distributions were asymmetric (Fig. S1) and thus the median was a more robust parameter than the mean [27]. The variance $\sigma^2(g)$ was estimated through a bootstrap procedure [50] based on 1000 bootstrap replications.

In order to test if the medians of different data groups were significantly different, we performed a hypothesis test. The P-values are obtained as follows:

$$P\text{-value} = 2\left[1 - F\left(\frac{|med(g1) - med(g2)|}{\sqrt{\sigma^2(g1) + \sigma^2(g2)}}\right)\right] \quad (3)$$

where F is the standard normal distribution and g1 and g2 represent the data groups.

Statistical data analysis was performed using the R software.

2.5. Numerical simulations

Numerical simulations were run using a tug-of-war model [48,51–55] as described in Supplementary Data. Briefly, the model considers a cargo driven by teams of opposed-polarity motors (i.e. kinesins and dyneins). The interaction of the motors with the cargo is assumed to be elastic, i.e. the motors and associated adaptor proteins act as parallel springs with elastic constant Ko. The motors move in discrete 8-nm steps along the microtubule, with load-dependent probabilities of stepping and detachment. Detached motors can stochastically rebind the microtubule track. The parameters used in these simulations were those described in Table S1.

The simulated trajectories (time step = 10 μs) were resampled to 3 ms and analyzed following the procedures previously described for those obtained experimentally.

3. Results and discussion

To study the mechanical properties of the motor-complex linker attaching melanosomes of different sizes, we treated melanophore cells with latrunculin to depolymerize the actin network and stimulated the cells for either aggregation or dispersion. In a previous work [4], we showed that 74% of the organelles move toward the microtubules plus-end during dispersion while this population is reduced to 40% in aggregation. Also, plus-end directed melanosomes were more prone to switch their direction reflecting the different performance of dynein and kinesin-2 motors during melanosome transport. In that previous work we also showed that the reversion probability for dynein-driven organelles increased during dispersion (from 0.17 to 0.25) whereas it slightly decreases for kinesin-2 driven organelles (from 0.46 to 0.41).

We performed SPT experiments and obtained trajectories of melanosomes with high temporal and spatial resolution (3 ms and 4–7 nm, respectively), Fig. 1 schematically shows the methodology applied to determine κ. Briefly, we extracted regions of the trajectories showing processive motion and split them into segments of 130 data points (390 ms). These segments were fitted with a second order polynomial function to define the main transport axis and were further decomposed into parallel ($x//$) and perpendicular ($y_\perp$) motion with respect to the transport axis (Fig. 1b). This last component was used to determine the effective elastic constant of the motor linker while $x//$ was used to compute the organelle speed.

In addition, we determined the optical radius (r_{op}) of melanosomes as described in [26]; in that previous work we also showed that r_{op} is linearly related to the organelle radius within the assayed range.

Fig. 2a–b shows the median values of speed and stiffness (regardless of the overall direction of the organelles in the segments) obtained during aggregation and dispersion as a function of the organelle size. The figure shows that the stiffness of the linker increases with the organelle size while the speed followed the opposite behavior. Moreover, the stimulation condition affects these behaviors indicating that they are influenced by the motors involved in the transport and thus could not be only assigned to the drag introduced by the media. Supporting this conclusion, we run numerical simulations and also found that an increasing drag reduces the speed of the organelles but it does not affect the value of κ (Fig. S2). The values of speed determined in this work are in the order of those reported for the motors in in vitro conditions (0.7 μm/s and 0.58 μm/s for dynein–dynactin and kinesin-2, respectively [45,56]) and for purified melanosomes (1.15 μm/s and 0.65 μm/s for minus and plus directed organelles, [49]).

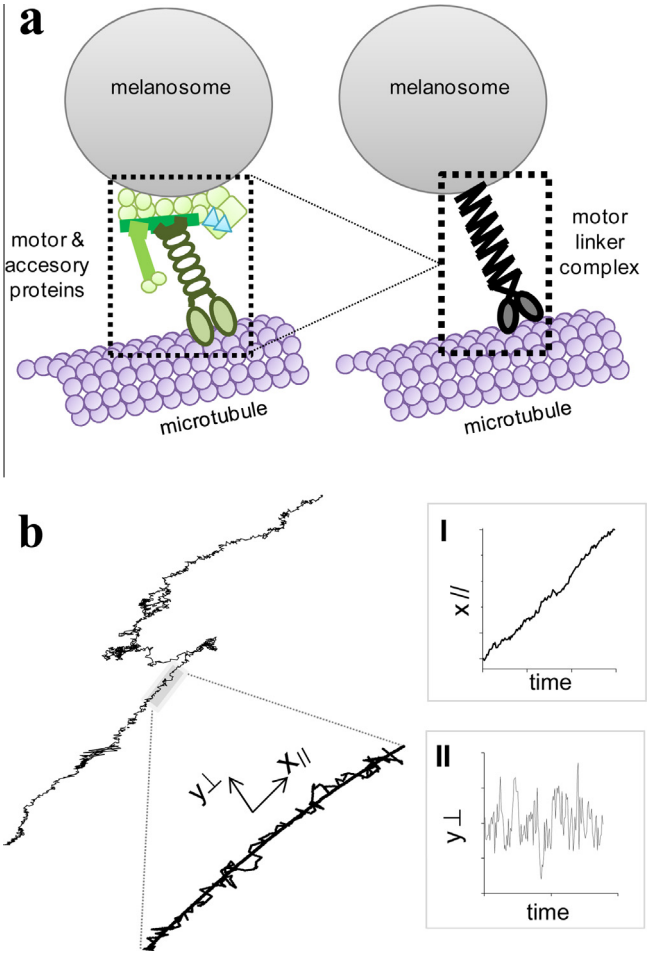

Fig. 1. Analysis of trajectories. Molecular motors and accessory proteins attached to the melanosome established a spring-like interaction with the microtubule (a). The trajectories of organelles were split into curvilinear segments of 0.39 s which were fit with a second order polynomial function to define the transport direction (b). The segments were decomposed into parallel ($x//$) and perpendicular ($y_\perp$) motion with respect to the direction axis to study the melanosome dynamics.

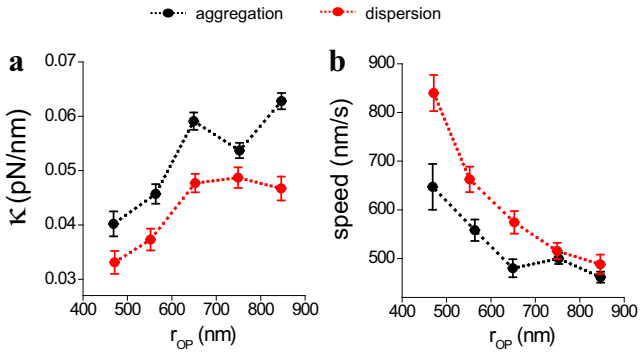

Fig. 2. Dependence of κ and speed on melanosomes size. The trajectories of melanosomes were registered during aggregation (●) or dispersion (●) and analyzed as described in the text to compute the values of the effective elastic constant (κ) and the speed. The radii data were grouped in bins of 100 nm and the median value of κ (a) and speed (b) obtained for each bin was plotted as a function of the mean radius in each interval (Ndata = 150–600 for each bin). The error bars represent the standard error.

We have previously mentioned recent evidences suggesting that the transport of bigger organelles require the action of multiple copies of motors. In this context, our results could be explained

considering that each of these active motor-complexes contributes as parallel springs to the value of κ In the same direction Efremov et al. [36] observed that the position fluctuations of peroxisomes (inversely related to κ) transported by kinesin motors decreases when more motors are recruited to their surfaces and engaged in transport. Numerical simulations also confirmed that the stiffness of the linker increases with the number of motors (Fig. S2). Despite our data does not provide direct information regarding the number of motors attached to different-sized organelles, it suggests that this dependence is not linear. We can hypothesize that the curvature radius of organelles may impose some geometrical restrictions to this dependence. A higher curvature (i.e. smaller organelle) would imply that fewer motors will be close enough to the microtubule to attach to it (Supplementary data).

In order to understand the relative contributions of dynein and kinesin motors to the observed behavior we classified the trajectory segments according to the main transport direction – i.e. toward the cell nucleus or away from it – in both stimulation conditions and analyzed the behavior of the subpopulations of the relatively small (400–600 nm) and big (700–900 nm) organelles. This classification was done taking into account the apparent different behavior of these populations observed in Fig. 2a and our previous work showing that the tortuosity of melanosome trajectories decreases with the organelle size reaching a constant value for organelles with $r_{op} > 600$ nm [26].

Fig. 3 shows that whereas the overall dependence of both κ and speed on the organelle radius is similar to those observed in Fig. 2, dynein and kinesin-driven organelles present a very different behavior.

Organelles moving toward the plus-end present higher values of κ in aggregation with respect to dispersion (Fig. 3a). These results suggest that dynein motors – more active during aggregation – link the organelle to the microtubule even if the cargo is moving toward the microtubule plus-end. The involvement of these motors in a tug-of-war with kinesin also slows down small cargoes transported toward the plus-end in aggregation (Fig. 3b).

On the other hand, kinesin motors do not seem to affect the motion of minus-end directed organelles since the dependence of their speed and stiffness with the radius was the same in both stimulation conditions (Fig. 3d). These results suggest that either kinesin-2 is inactive during minus-end transport or its activity remains constant in aggregation and dispersion.

Fig. 3 also shows that the speed of big organelles were insensitive to the stimulation condition suggesting that the drag limits their motion during both plus and minus-end directed transport. According to previous works, it is expected that a relatively large number of motors pull the cargo against the opposing force when the drag is high [57,58].

The dissimilar behavior of dynein and kinesin-driven organelles indicate that these motors play a different role in transport: whereas the presence of dynein clearly affects the evaluated properties of kinesin-driven organelles, the opposite does not seem to be true.

In a recent work Blehm et al. [59] measured the in vivo stall forces of lipid droplets and found that cytoplasmic dynein is active during both minus- and plus-end directed motion whereas kinesin is only active in the plus-end direction. Also, Schroeder et al. [60] measured the biophysical properties of kinesin-2 and showed that this motor is less processive and more prone to detach than kinesin-1 under load even though their stall forces were similar (~5 pN). Despite these experiments were not performed in melanophores cells, they provide evidences supporting a model in which kinesin-2 is not engaged to the microtubule during minus-end transport.

Our results could be explained with the model depicted in Fig. 4. This figure includes possible, mean configurations of plus and minus motors attached to either relative small or big organelles during aggregation and dispersion. We should point out that this scheme is speculative since, as far as we know, the number of motors attached to melanosomes remains unknown. Moreover, the proposed simplified model does not include higher levels of transport regulation that may affect motor properties and the different

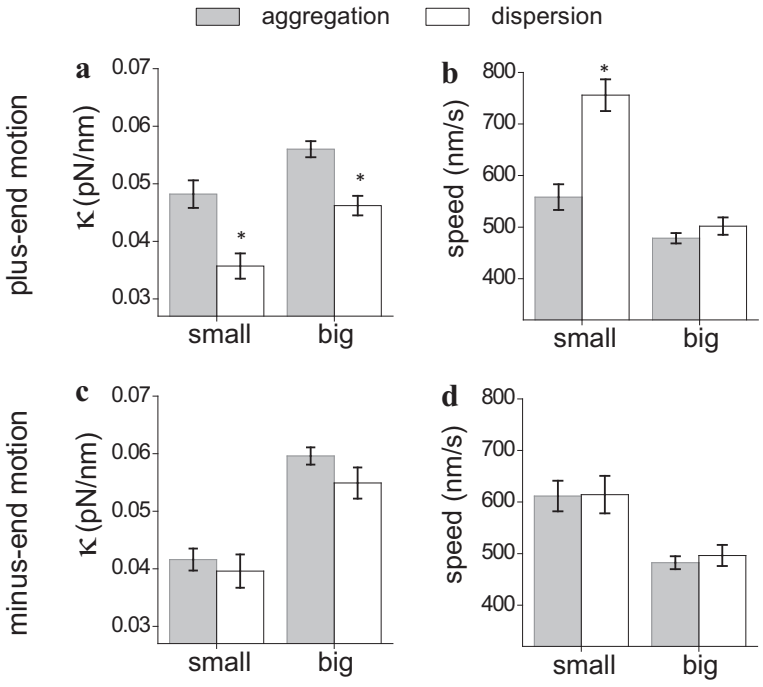

Fig. 3. Stiffness and speed of melanosomes transported by kinesin-2 and dynein. Kinesin-2 (a–b) and dynein (c–d) runs during aggregation (gray bars) and dispersion (white bars) were analyzed and divided into small and big organelles as described in the text. The data is expressed as medians (*N*data = 150–600 in each bin). The error bars represents the standard error of the κ and speed determination in each group.

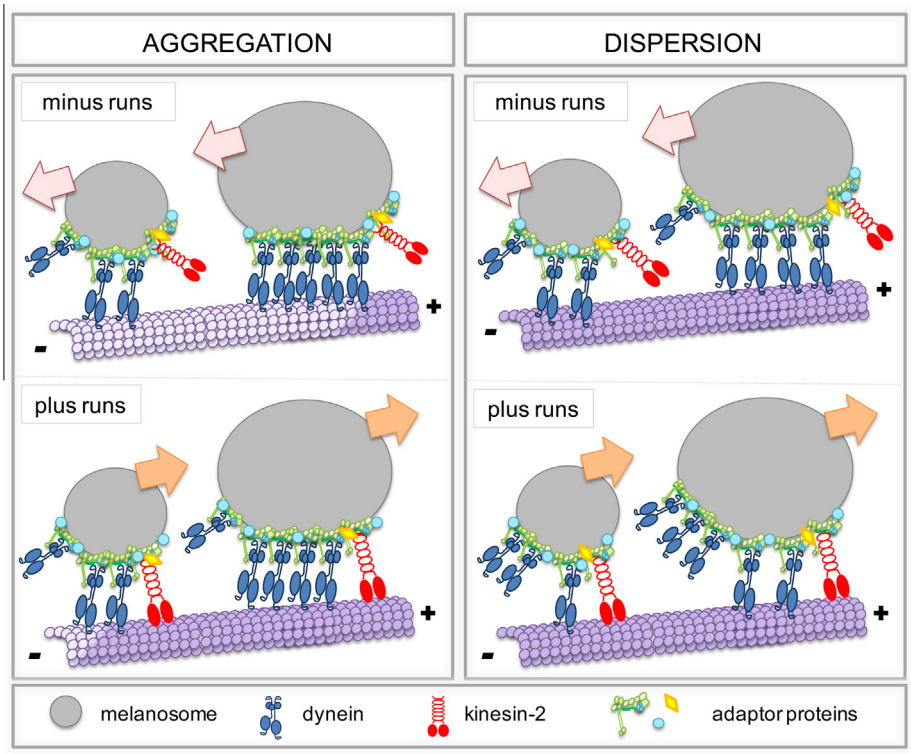

Fig. 4. Schematic representation of microtubule transport of small and big melanosomes during aggregation (left panel) and dispersion (right panel). The scheme represents different configurations of motors attached to small and big melanosomes moving toward the minus (top panels) or plus-end (bottom panels) of the microtubule. The motors depicted in the drawing do not represent the real number of motors engaged in melanosome transport.

motor configurations resulting from the local tug of war in each condition.

We considered evidences described in the literature suggesting that cargoes are transported by several dynein copies against a single kinesin [12]. In that previous work, cargoes were driven by cytoplasmic dynein and DdUnc-104 kinesin, thus we cannot assure that kinesin-2 behaves similarly when transporting melanosomes. The scheme also shows that big organelles attach more motor copies agreeing with previous results [26]. In addition, we considered that the number of motors attached to melanosomes do not change with the stimulation condition as determined by Gross et al. [25] whereas the number of motors engaged in transport is affected by hormone treatment.

According to our simplified model, kinesin disengaged from the track during minus-end runs whereas dynein motors remain attached to the microtubule during plus-end runs.

During aggregation, the minus-end transport of melanosomes is achieved by the increased activity of dyneins (e.g. more dyneins attached to the track). The stochastic attachment of kinesin-2 results in an asymmetric tug-of-war between these opposite-polarity motors; when force exerted in the plus-end direction is higher the organelle revers its movement direction. We hypothesize that the linker stiffness increases with the number of motors anchored to the microtubule and thus κ increases for plus-end moving organelles.

On the other hand, the mean number of dynein motors attached to the track decreases during dispersion and thus the probability of plus-end runs increases. As a consequence, κ values determined for plus-end organelles are smaller than those measured during aggregation. Also, the speed of small plus-end moving organelles increases due to a lower dynein-drag.

In conclusion, our results suggest that dynein motors compete with kinesin-2 during melanosome transport affecting the properties of plus-end directed organelles whereas kinesin-2 does not seem to affect minus-end transport.

Acknowledgments

This research was supported by ANPCyT (PICT 2012-0899, PICT-2012-1641) and UBACyT (20020110100074, 20020120200244) and CONICET (PIP 11220110100742). VL, MEDR, MS, DR and LB are members of CONICET.

Appendix A. Supplementary data

Supplementary data associated with this article can be found, in the online version, at http://dx.doi.org/10.1016/j.febslet.2015.07.038.

References

[1] Mallik, R. and Gross, S.P. (2004) Molecular motors: strategies to get along. Curr. Biol. 14, R971–R982.
[2] Vale, R.D. (2003) The molecular motor toolbox for intracellular transport. Cell 112, 467–480.
[3] Ishii, Y. and Yanagida, T. (2003) Single molecule measurements and molecular motors in: Molecular motors (Schliwa, M., Ed.), Wiley-VCH, Munchen.
[4] Bruno, L., Echarte, M.M. and Levi, V. (2008) Exchange of microtubule molecular motors during melanosome transport in *Xenopus laevis* melanophores is triggered by collisions with intracellular obstacles. Cell Biochem. Biophys. 52, 191–201.
[5] Brunstein, M., Bruno, L., Desposito, M. and Levi, V. (2009) Anomalous dynamics of melanosomes driven by myosin-V in *Xenopus laevis* melanophores. Biophys. J. 97, 1548–1557.
[6] Levi, V., Gelfand, V.I., Serpinskaya, A.S. and Gratton, E. (2006) Melanosomes transported by myosin-V in *Xenopus melanophores* perform slow 35 nm steps. Biophys. J. 90, L07–L09.
[7] Levi, V., Serpinskaya, A.S., Gratton, E. and Gelfand, V. (2006) Organelle transport along microtubules in *Xenopus melanophores*: evidence for cooperation between multiple motors. Biophys. J. 90, 318–327.

[8] Hendricks, A.G., Perlson, E., Ross, J.L., Schroeder 3rd, H.W., Tokito, M. and Holzbaur, E.L. (2010) Motor coordination via a tug-of-war mechanism drives bidirectional vesicle transport. Curr. Biol. 20, 697–702.
[9] Gross, S.P., Welte, M.A., Block, S.M. and Wieschaus, E.F. (2002) Coordination of opposite-polarity microtubule motors. J. Cell Biol. 156, 715–724.
[10] Fu, M.M. and Holzbaur, E.L. (2013) JIP1 regulates the directionality of APP axonal transport by coordinating kinesin and dynein motors. J. Cell Biol. 202, 495–508.
[11] Laib, J.A., Marin, J.A., Bloodgood, R.A. and Guilford, W.H. (2009) The reciprocal coordination and mechanics of molecular motors in living cells. Proc. Natl. Acad. Sci. U.S.A. 106, 3190–3195.
[12] Soppina, V., Rai, A.K., Ramaiya, A.J., Barak, P. and Mallik, R. (2009) Tug-of-war between dissimilar teams of microtubule motors regulates transport and fission of endosomes. Proc. Natl. Acad. Sci. U.S.A. 106, 19381–19386.
[13] Blehm, B.H. and Selvin, P.R. (2014) Single-molecule fluorescence and in vivo optical traps: how multiple dyneins and kinesins interact. Chem. Rev. 114, 3335–3352.
[14] Nascimento, A.A., Roland, J.T. and Gelfand, V.I. (2003) Pigment cells: a model for the study of organelle transport. Annu. Rev. Cell Dev. Biol. 19, 469–491.
[15] Rozdzial, M.M. and Haimo, L.T. (1986) Bidirectional pigment granule movements of melanophores are regulated by protein phosphorylation and dephosphorylation. Cell 47, 1061–1070.
[16] Sammak, P.J., Adams, S.R., Harootunian, A.T., Schliwa, M. and Tsien, R.Y. (1992) Intracellular cyclic AMP not calcium, determines the direction of vesicle movement in melanophores: direct measurement by fluorescence ratio imaging. J. Cell Biol. 117, 57–72.
[17] Kashina, A. and Rodionov, V. (2005) Intracellular organelle transport: few motors, many signals. Trends Cell Biol. 15, 396–398.
[18] Ikeda, K., Zhapparova, O., Brodsky, I., Semenova, I., Tirnauer, J.S., Zaliapin, I. and Rodionov, V. (2011) CK1 activates minus-end-directed transport of membrane organelles along microtubules. Mol. Biol. Cell 22, 1321–1329.
[19] Reilein, A.R., Tint, I.S., Peunova, N.I., Enikolopov, G.N. and Gelfand, V.I. (1998) Regulation of organelle movement in melanophores by protein kinase A (PKA), protein kinase C (PKC), and protein phosphatase 2A (PP2A). J. Cell Biol. 142, 803–813.
[20] Kashina, A.S., Semenova, I.V., Ivanov, P.A., Potekhina, E.S., Zaliapin, I. and Rodionov, V.I. (2004) Protein kinase A, which regulates intracellular transport, forms complexes with molecular motors on organelles. Curr. Biol. 14, 1877–1881.
[21] Deacon, S.W., Nascimento, A., Serpinskaya, A.S. and Gelfand, V.I. (2005) Regulation of bidirectional melanosome transport by organelle bound MAP kinase. Curr. Biol. 15, 459–463.
[22] Nilsson, H. and Wallin, M. (1997) Evidence for several roles of dynein in pigment transport in melanophores. Cell Motil. Cytoskeleton 38, 397–409.
[23] Tuma, M.C., Zill, A., Le Bot, N., Vernos, I. and Gelfand, V. (1998) Heterotrimeric kinesin II is the microtubule motor protein responsible for pigment dispersion in *Xenopus melanophores*. J. Cell Biol. 143, 1547–1558.
[24] Rogers, S.L., Karcher, R.L., Roland, J.T., Minin, A.A., W., S. and Gelfand, V.I. (1999) Regulation of melanosome movement in the cell cycle by reversible association with myosin V. J. Cell Sci. 146, 1265–1276.
[25] Gross, S.P., Tuma, M.C., Deacon, S.W., Serpinskaya, A.S., Reilein, A.R. and Gelfand, V.I. (2002) Interactions and regulation of molecular motors in *Xenopus melanophores*. J. Cell Biol. 156, 855–865.
[26] De Rossi, M.C., Bruno, L., Wolosiuk, A., Desposito, M.A. and Levi, V. (2013) When size does matter: organelle size influences the properties of transport mediated by molecular motors. Biochim. Biophys. Acta 1830, 5095–5103.
[27] Fu, M.M. and Holzbaur, E.L. (2014) Integrated regulation of motor-driven organelle transport by scaffolding proteins. Trends Cell Biol. 24, 564–574.
[28] Kural, C., Kim, H., Syed, S., Goshima, G., Gelfand, V.I. and Selvin, P.R. (2005) Kinesin and dynein move a peroxisome in vivo: a tug-of-war or coordinated movement? Science 308, 1469–1472.
[29] Semenova, I. et al. (2014) Regulation of microtubule-based transport by MAP4. Mol. Biol. Cell 25, 3119–3132.
[30] Hill, D.B., Plaza, M.J., Bonin, K. and Holzwarth, G. (2004) Fast vesicle transport in PC12 neurites: velocities and forces. Eur. Biophys. J. 33, 623–632.
[31] Luby-Phelps, K., Castle, P.E., Taylor, D.L. and Lanni, F. (1987) Hindered diffusion of inert tracer particles in the cytoplasm of mouse 3T3 cells. Proc. Natl. Acad. Sci. U.S.A. 84, 4910–4913.
[32] Bursac, P., Lenormand, G., Fabry, B., Oliver, M., Weitz, D.A., Viasnoff, V., Butler, J.P. and Fredberg, J.J. (2005) Cytoskeletal remodelling and slow dynamics in the living cell. Nat. Mater. 4, 557–561.
[33] Fabry, B., Maksym, G.N., Butler, J.P., Glogauer, M., Navajas, D. and Fredberg, J.J. (2001) Scaling the microrheology of living cells. Phys. Rev. Lett. 87, 148102.
[34] Lau, A.W., Hoffman, B.D., Davies, A., Crocker, J.C. and Lubensky, T.C. (2003) Microrheology, stress fluctuations, and active behavior of living cells. Phys. Rev. Lett. 91, 198101.
[35] Mason, T.G. and Weitz, D.A. (1995) Optical measurements of frequency-dependent linear viscoelastic moduli of complex fluids. Phys. Rev. Lett. 74, 1250–1253.
[36] Efremov, A.K., Radhakrishnan, A., Tsao, D.S., Bookwalter, C.S., Trybus, K.M. and Diehl, M.R. (2014) Delineating cooperative responses of processive motors in living cells. Proc. Natl. Acad. Sci. U.S.A. 111, E334–E343.
[37] Bandyopadhyay, D., Cyphersmith, A., Zapata, J.A., Kim, Y.J. and Payne, C.K. (2014) Lysosome transport as a function of lysosome diameter. PLoS One 9, e86847.
[38] Bhat, D. and Gopalakrishnan, M. (2012) Effectiveness of a dynein team in a tug of war helped by reduced load sensitivity of detachment: evidence from the study of bidirectional endosome transport in *D. discoideum*. Phys. Biol. 9, 046003.
[39] Bryantseva, S.A. and Zhapparova, O.N. (2012) Bidirectional transport of organelles: unity and struggle of opposing motors. Cell Biol. Int. 36, 1–6.
[40] Schliwa, M. and Woehlke, G. (2003) Molecular motors. Nature 422, 759–765.
[41] Schroer, T.A. (2004) Dynactin. Annu. Rev. Cell Dev. Biol. 20, 759–779.
[42] Vallee, R.B., McKenney, R.J. and Ori-McKenney, K.M. (2012) Multiple modes of cytoplasmic dynein regulation. Nat. Cell Biol. 14, 224–230.
[43] Deacon, S.W., Serpinskaya, A.S., Vaughan, P.S., Lopez Fanarraga, M., Vernos, I., Vaughan, K.T. and Gelfand, V.I. (2003) Dynactin is required for bidirectional organelle transport. J. Cell Biol. 160, 297–301.
[44] Kardon, J.R. and Vale, R.D. (2009) Regulators of the cytoplasmic dynein motor. Nat. Rev. Mol. Cell Biol. 10, 854–865.
[45] Berezuk, M.A. and Schroer, T.A. (2007) Dynactin enhances the processivity of kinesin-2. Traffic 8, 124–129.
[46] Tripathy, S.K., Weil, S.J., Chen, C., Anand, P., Vallee, R.B. and Gross, S.P. (2014) Autoregulatory mechanism for dynactin control of processive and diffusive dynein transport. Nat. Cell Biol. 16, 1192–1201.
[47] Bruno, L., Salierno, M., Wetzler, D.E., Desposito, M.A. and Levi, V. (2011) Mechanical properties of organelles driven by microtubule-dependent molecular motors in living cells. PLoS One 6, e18332.
[48] Bouzat, S., Levi, V. and Bruno, L. (2012) Transport properties of melanosomes along microtubules interpreted by a tug-of-war model with loose mechanical coupling. PLoS One 7, e43599.
[49] Rogers, S.L., Tint, I.S., Fanapour, P.C. and Gelfand, V.I. (1997) Regulated bidirectional motility of melanophore pigment granules along microtubules in vitro. Proc. Natl. Acad. Sci. U.S.A. 94, 3720–3725.
[50] Wasserman, L. (2010) All of Statistics: a Concise Course in Statistical Inference, Springer-Verlag, New York.
[51] Muller, M.J., Klumpp, S. and Lipowsky, R. (2010) Bidirectional transport by molecular motors: enhanced processivity and response to external forces. Biophys. J. 98, 2610–2618.
[52] Kunwar, A. and Mogilner, A. (2010) Robust transport by multiple motors with nonlinear force-velocity relations and stochastic load sharing. Phys. Biol. 7, 16012.
[53] Kunwar, A. et al. (2011) Mechanical stochastic tug-of-war models cannot explain bidirectional lipid-droplet transport. Proc. Natl. Acad. Sci. U.S.A. 108, 18960–18965.
[54] Kunwar, A., Vershinin, M., Xu, J. and Gross, S.P. (2008) Stepping, strain gating, and an unexpected force-velocity curve for multiple-motor-based transport. Curr. Biol. 18, 1173–1183.
[55] Bouzat, S. and Falo, F. (2010) The influence of direct motor–motor interaction in models for cargo transport by a single team of motors. Phys. Biol. 7, 046009.
[56] King, S.J. and Schroer, T.A. (2000) Dynactin increases the processivity of the cytoplasmic dynein motor. Nat. Cell Biol. 2, 20–24.
[57] Hendricks, A.G., Holzbaur, E.L. and Goldman, Y.E. (2012) Force measurements on cargoes in living cells reveal collective dynamics of microtubule motors. Proc. Natl. Acad. Sci. U.S.A. 109, 18447–18452.
[58] Nam, W. and Epureanu, B.I. (2015) Highly loaded behavior of kinesins increases the robustness of transport under high resisting loads. PLoS Comput. Biol. 11, e1003981.
[59] Blehm, B.H., Schroer, T.A., Trybus, K.M., Chemla, Y.R. and Selvin, P.R. (2013) In vivo optical trapping indicates kinesin's stall force is reduced by dynein during intracellular transport. Proc. Natl. Acad. Sci. U.S.A. 110, 3381–3386.
[60] Schroeder 3rd, H.W., Hendricks, A.G., Ikeda, K., Shuman, H., Rodionov, V., Ikebe, M., Goldman, Y.E. and Holzbaur, E.L. (2012) Force-dependent detachment of kinesin-2 biases track switching at cytoskeletal filament intersections. Biophys. J. 103, 48–58.